J Mater Sci: Mater Electron (2017) 28:14499–14503
DOI 10.1007/s10854-017-7313-8

Surface and optical properties of transparent Li_3PO_4 thin films deposited by magnetron sputtering technique

H. Hakan Yudar[1] · Suat Pat[1] · Şadan Korkmaz[1] · Soner Özen[1] · Zerrin Pat[2]

Received: 23 April 2017 / Accepted: 6 June 2017 / Published online: 10 June 2017

Abstract Li_3PO_4 materials are widely used as a solid electrolyte for the all-solid-state battery, electrochromic and optoelectronic devices including ion conductor layer. Li_3PO_4 thin films were deposited on glass substrates by RF magnetron sputtering system at argon atmosphere. Surface and optical properties of the Li_3PO_4 thin films were investigated by some analysis techniques. Scanning electron and atomic force microscope were used to determine of the surface morphologies of produced Li_3PO_4 thin films. Absorbance and transmittance spectra were recorded using UV–Vis spectrophotometer in the range of 200–1000 nm. The absorbance values were approximately 0.05. The transmittance values were around 88 and 85% for *S1* and *S2* at 550 nm. The film thickness values of samples were 60 and 90 nm. The reflectance spectra values of the Li_3PO_4 were about 5.9 and 6.4% at 550 nm for *S1* and *S2*, respectively. The refractive index values of the Li_3PO_4 were measured as approximately 1.59.

1 Introduction

Nowadays, the lithium-ion batteries (LiBs) play important role in all the rechargeable battery market. They have high energy [1] and power densities [2]. The LiB have been used for variously portable equipment [3]. The main elements of the battery are the cathode [4–6], the anode [7–9] and the electrolyte [10, 11]. The electrolyte layer of the battery is an important role in the LiB's performance.

A liquid or gel electrolytes are used to in LiB for Li-ion transport between the electrode layers. The traditional LiB systems are not sufficient to meet the growing storage demands of the micro and nano devices power systems. The traditional system has unsafely, short cycle life, low power density, and the high working temperature. Other disadvantages are the battery dimensions and mass. Liquid or gel contains batteries has a bigger dimension and mass according to the thin film battery (TFB). TFB is a fully solid-state battery. TFB contains all-solid-state electrolyte for Li-transfer. For these reasons, research has begun on the use of solid electrolytes with high ionic conductivity for TFB in recent years. These new generations TFB is also titled to as all-solid-state battery (SSB). The SSBs have the features such as nano-structured composites [12], high power density [13], long cycle life [14], high-rate capability [15], high performance [16] and excellent safety operation [17]. SSBs have been studied in recent years because of their potential applications in microelectronics, communications, smart cards, and medical devices. In SSBs, the solid electrolyte plays critical role. Hence, high ionic conductivity materials are used to. Li_3PO_4 is relatively high ionic conductor material among the solid electrolyte for the SSBs. Also, this layer is widely used in all-solid-state electrochromic and optoelectronic devices. Li_3PO_4 layers work as also separator material. In SSBs, a Li_3PO_4 films can be deposited by the various methods such as RF magnetron sputtering [18], solid-state reaction [19], chemical precipitation [20], wet chemical [21], spray coating [1], pulsed laser deposition [22], thermal evaporation [23], electrostatic spray deposition [24], ion beam sputtering deposition, and etc. The RF magnetron sputtering process is a preferred technique

✉ Suat Pat
suatpat@ogu.edu.tr

[1] Art and Science Faculty, Eskişehir Osmangazi University, Eskişehir, Turkey

[2] Art and Science Faculty, Bilecik University, Bilecik, Turkey

owing to the reproducibility, high deposition rate, easy setting of parameters and film quality. RF magnetron sputtering techniques also used in commercial SSB productions.

The performance value of the all-solid-state battery is related with the microstructural and surface properties of the layers [25–28]. Solid electrolyte is key materials for the all-solid-state battery. Three types solid electrolytes, including oxides, oxynitrides and sulphides, were used. In this paper, surface and optical properties of the deposited transparent Li_3PO_4 thin films for by RF magnetron sputtering technique for generating high transparent all-solid-state battery. Any annealing process was not carried out for substrates. The optical and surface properties of the Li_3PO_4 films were investigated for electrolyte layer of the SSB. The surface imaging and characterizations of the Li_3PO_4 were determined using scanning electron microscopy (SEM) and atomic force microscopy (AFM). An UV–Vis spectrophotometer in the range of 200–1000 nm was used to determine the optical properties of the deposited Li_3PO_4 layers for transparent electrolyte layer of the SSBs and all-solid-state electrochromic (SSE) devices. These analyze show that the transparent solid electrolyte layers for SSBs and SSE can be manufactured by RF technology.

Table 1 Deposition parameters for samples

Parameters (Unit)	Sample 1 (*S1*)	Sample 2 (*S2*)
Pressure (Torr)	6×10^{-2}	6×10^{-2}
Power (Watt)	80	80
Duration (min)	30	80
Gas (–)	Argon	Argon

2 Experimental

The Li_3PO_4 thin films were deposited using RF magnetron sputter technique. Before the Li_3PO_4 thin films produced, the glass substrates were cleaned de-ionized water for 5 min. The cleaned glasses were allowed dried in air for 30 min. The Li_3PO_4 target was used. The Li_3PO_4 target have high purity. Target diameter is 2 inches and thickness of the disc 0.125 inches. The distance between the substrates and the target was 50 mm. The vacuum pressure of the chamber was approximately 1×10^{-3} Torr before the started the process. Argon gas (99.99%) was used for the process gas. The deposition pressures were adjusted to 6×10^{-2} Torr for the samples. RF deposition power was kept constant. The deposition parameters of the experiment are summarized in Table 1.

3 Results and discussion

SEM and AFM tools were used for the surface properties of the Li_3PO_4 thin films. The SEM surface topography of Li_3PO_4 thin films coated on glass substrates is shown in Fig. 1. JEOL JSM 5600 was used for SEM images of samples. The images of Li_3PO_4 thin films were presented with a magnification of ×15k times for each two sample in the Fig. 1a, b. The coated Li_3PO_4 are seen in the Fig. 1a, b. The morphologies of coated surface are smooth and uniform in Fig. 1a, b. Crystalline structures can manage to imaging for *S1* sample, shown in Fig. 1a.

The AFM (Ambios Q-Scope) device was used to obtain the two and three-dimensional images of surface morphology of samples. The Scan Atomic V 5.1.0 SPM control software was operated in non-contact mode. The surface features of the Li_3PO_4 thin films were investigated using the AFM over 4×4 m^2 scanning areas. In the measurements,

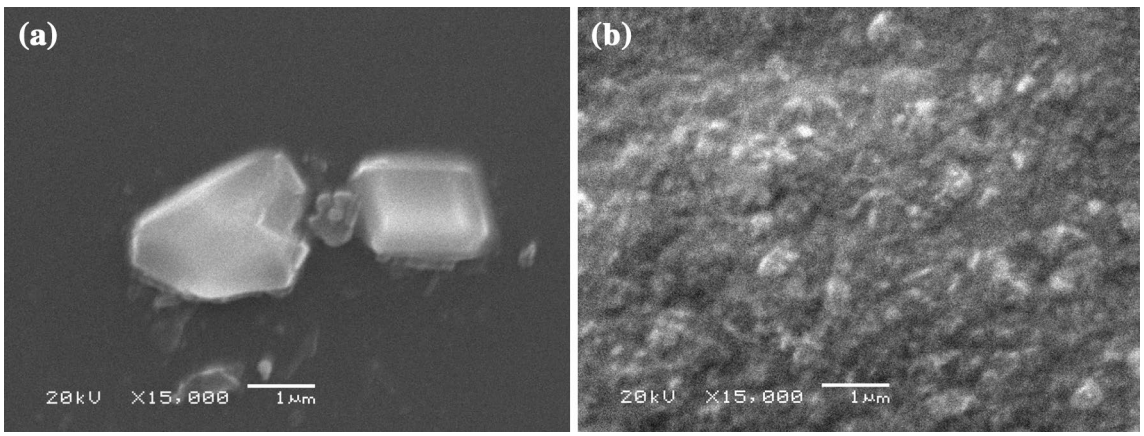

Fig. 1 SEM images of Li_3PO_4 thin films for **a** *S1* and **b** *S2* samples

scan angle and scan rates had 0° and 8 Hz at the AFM, respectively. The AFM images of the surfaces of the films are shown in 2D and 3D for *S1* and *S2* in Fig. 2a, b. Obtained images are looks like to SEM images, illustrated in Fig. 1a, b.

Using AFM, the root means square roughness (RMS), Skewness (Ssk), Kurtosis (Skr) was determined at high resolution. The RMS is an important parameter to describe the surface roughness due to represent the standard deviation of the surface height distribution. The RMS parameter is average height. The Skewness (Ssk) means to measure and understand the asymmetry of the height distribution of the samples. The Kurtosis (Skr) is to measure and understand the smoothness of the samples. The measured RMS values of samples are as approximate 1.93 and 56.8 nm for S_1 and S_2, respectively. These Ssk values demonstrate a perfectly symmetrical grain distribution on the surface. The value of Ssk is equal to zero in ideally. But, the value can shift to a positive or negative value. The positive value for Ssk means that height distribution on the sample surface is an asymmetric form. The Ssk is a measure of the sharpness of the roughness profile. As a result, the obtained Ssk values of produced samples were 4.73, and 0.58 for *S1* and *S2*, respectively. The ideal Skr values demonstrate a perfect normal distribution structure on the surface. The Skr may have a positive or negative value. The Skr positive value means that the peak distribution of surface structure is sharp. The Skr negative value means that the top distribution of surface structure is flat. Obtained Skr values of produced films were 36.22 and −0.43 for *S1* and *S2* at the scanned areas, respectively. According to these values, *S1* and *S2* have different surface structures. The surface structure of *S1* has low smooth, asymmetric and sharp peaks. The surface structure of *S2* has high roughness, asymmetric and flat peaks. While increased the film thickness, the porous structures and cracks of the film surface were increased. The absorbance, transmittance, refractive index, and the reflectance of the produced Li_3PO_4 layers are represented in Fig. 3. Absorbance and transmittance spectra of the films were measured with UV–Vis transmission spectroscopy (UNICO 4802 double beam) in the wavelength range of 200–1000 nm. Absorbance and transmittance spectra are given in Fig. 3a, b. These measurements were performed at room temperature. The absorbance values are 0.05 and 0.06 for *S1* and *S2* at 550 nm, respectively. The transmittance values are seen as approximately 88 and 85% for *S1* and *S2* at 550 nm, respectively. The refractive index (n) and the reflectance (R) spectra were measured by an interferometer. A Filmetrics F20 film thickness measurement system was used for the analysis.

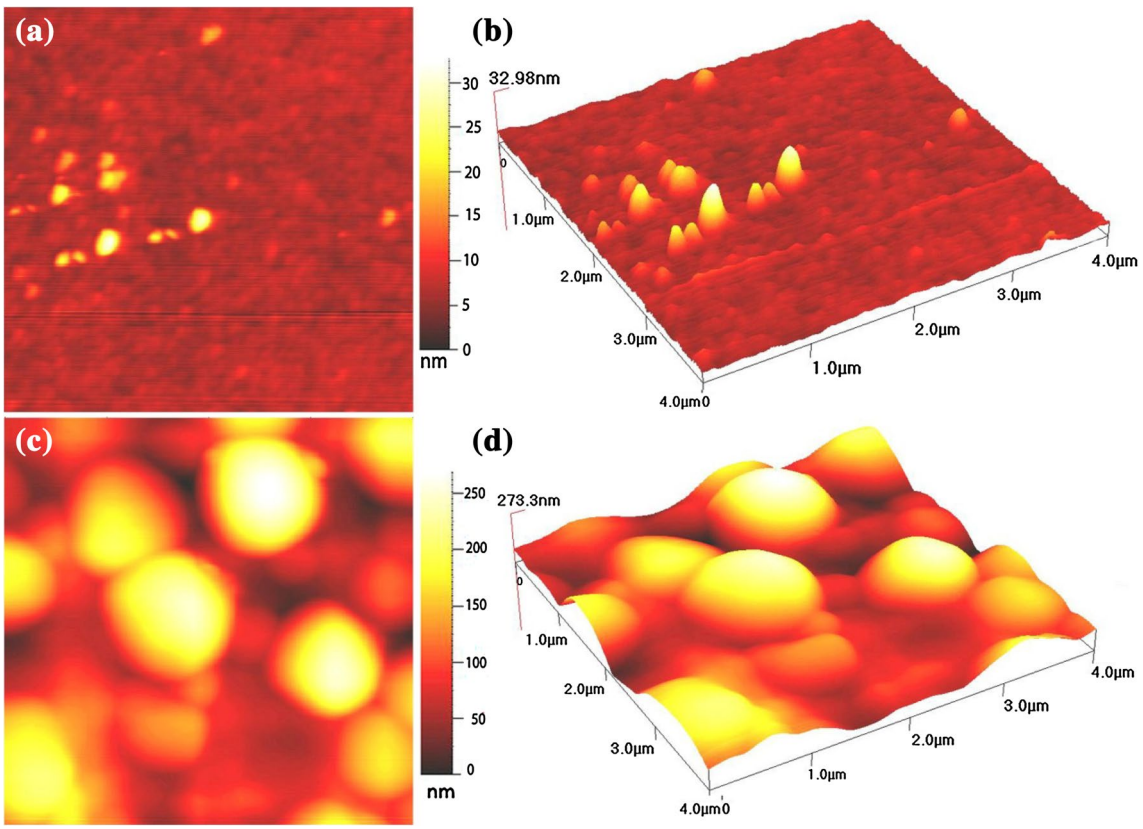

Fig. 2 2D and 3D AFM images of Li_3PO_4 thin films for (**a, b**) *S1* and (**c, d**) *S2*

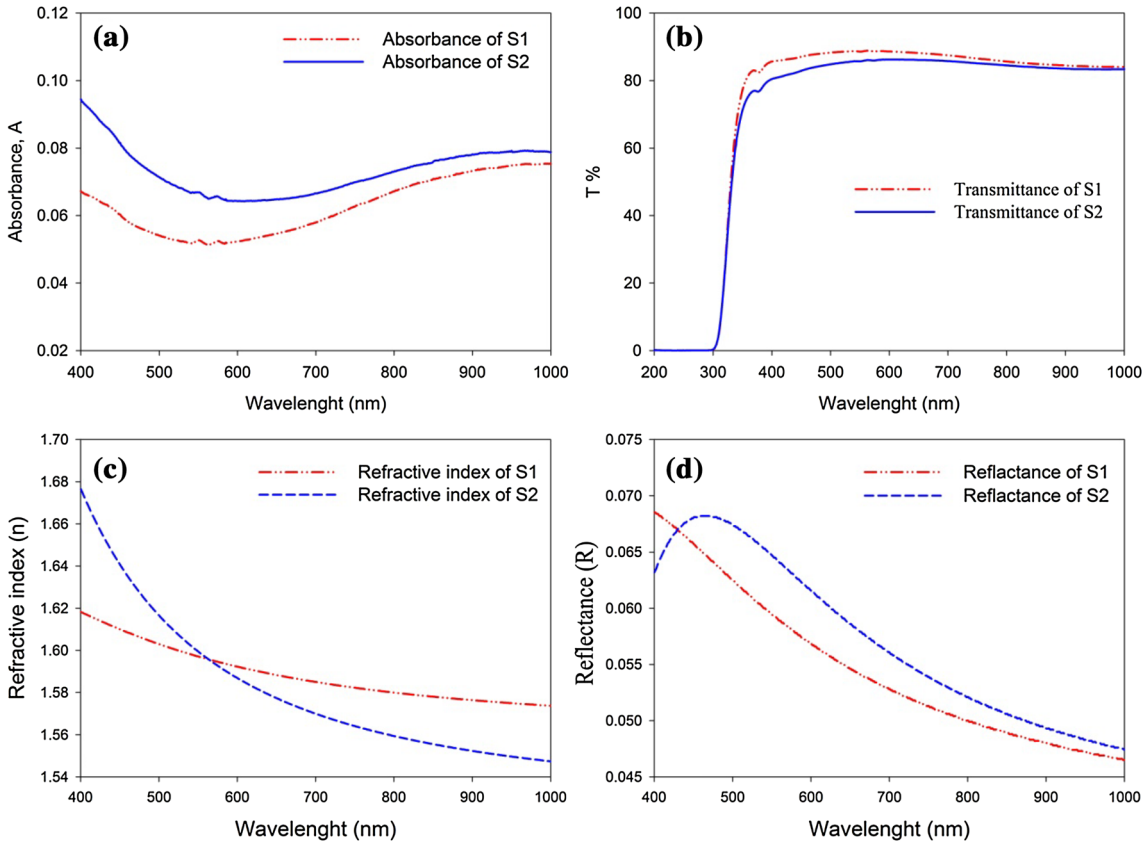

Fig. 3 **a** Absorbance, **b** transmittance, **c** refractive indices, and **d** reflectance graphs for *S1* and *S2*

These values are illustrated in Fig. 3c, d, respectively. The refractive index (n) spectra of the deposited samples were showed in Fig. 3c. The obtained values of refractive indices are in good agreement with samples produced by RF technique [29, 30]. The refractive index values of the coated films were approximately 1.6 for *S1* and *S2* at 550 nm. Increasing wavelength values, shown in the Fig. 3c, the refractive indices values decreases. For *S2* sample, film thickness is bigger than the thickness of the *S1* sample. But, transmittance value is nearly same due to the *S2* sample has bigger cracks and porosity. As result, refractive indices at lower frequencies are bigger than the value for the thinner sample *S1*. Porous films are better for the ion transportation in solid-state devices. The Li_3PO_4 is a wide band gap insulator with a band gap of 5.75 eV. The band gap of the deposited samples can be calculated using the value of refractive index [30]. The equation for this calculation is given as below:

$$n = \sqrt{\frac{12.417}{(E_g - 0.365)}} \quad (1)$$

where n and E_g are the refractive index and the optical band gap. If the refractive index values are taken as approximately 1.59 at 550 nm in Fig. 3c, the band gap values were calculated as 5.28 for each sample with Eq. 1. This value is very close the literature value. It was seen that the average reflectance values of coated samples were about 5.9 and 6.4% for *S1* and *S2* at 550 nm, respectively. In Fig. 3d, the reflectance (R) graph of produced samples is illustrated. Optical measurements are very important to determine the material properties [31].

4 Conclusions

Li_3PO_4 solid electrolyte layers have high ionic conductivity and a good separator for thin film battery (TFBs), solid-state battery (SSBs), and all-solid-state electrochromic (SSE) devices. In this paper, the Li_3PO_4 solid electrolyte was produced by the RF magnetron sputtering technique in the different production parameters. The optical and the surface properties of the Li_3PO_4 produced were analyzed. Li_3PO_4 layers affect the battery performance. The refractive index, the reflectance, the transmittance and the absorbance values have suitable for transparent layers. It was found

that deposited solid electrolytes layer are more proper for the transparent battery and electrochromic applications due to high transmittance value in the visible region. The deposited surfaces structures of the samples are smooth and compact. According to the obtained properties, the deposited layers can be used as the electrolyte layer for transparent thin film batteries and all-solid-state electrochromic devices.

Acknowledgements This research activity was supported by TUBITAK (Grant Number is 115E331).

References

1. Y. Kobayashi, S. Seki, A. Yamanaka, H. Miyashiro, Y. Mita, T. Iwahori, Development of high-voltage and high-capacity all-solid-state lithium secondary batteries. J. Power Sources **146**(1), 719–722 (2005)
2. M.S. Balogun, Z. Wu, Y. Luo, W. Qiu, X. Fan, B. Long, M. Hunag, P. Liu, Y. Tong, High power density nitridated hematite (α-Fe_2O_3) nanorods as anode for high-performance flexible lithium ion batteries. J. Power Sources **308**, 7–17 (2016)
3. J. Clement, Investigation of Thin Film Materials for Next Generation Lithium Ion Batteries, Doctoral dissertation (2016)
4. L.X. Yuan, Z.H. Wang, W.X. Zhang, X.L. Hu, J.T. Chen, Y.H. Huang, J.B. Goodenough, Development and challenges of $LiFePO_4$ cathode material for lithium-ion batteries. Energy Environ. Sci. **4**(2), 269–284 (2011)
5. M.Y. Saıdi, J. Barker, H. Huang, J.L. Swoyer, G. Adamson, Electrochemical properties of lithium vanadium phosphate as a cathode material for lithium-ion batteries. Electrochem. Solid-State Lett. **5**(7), A149–A151 (2002)
6. L. Zhou, D. Zhao, X.D. Lou, $LiNi_{0.5}Mn_{1.5}O_4$, Hollow structures as high-performance cathodes for lithium-ion batteries. Angew. Chem. **124**(1), 243–245 (2012)
7. E.F. Rodriguez, F. Xia, D. Chen, A.F. Hollenkamp, R.A. Caruso, N-doped $Li_4Ti_5O_{12}$ nanoflakes derived from 2D protonated titanate for high performing anodes in lithium ion batteries. J. Mater. Chem. A **4**(20), 7772–7780 (2016)
8. B. Li, X. Li, W. Li, Y. Wang, E. Uchaker, Y. Pei, G. Cao, Mesoporous tungsten trioxide polyaniline nanocomposite as an anode material for high-performance lithium-ion batteries. ChemNanoMat **2**(4), 281–289 (2016)
9. M. Kunduraci, Dealloying technique in the synthesis of lithium-ion battery anode materials. J. Solid State Electrochem. **20**(8), 2105–2111 (2016)
10. K. Thai, E. Lee, Elucidating the effects of additives on the lipon/electrode interface, with a focus on mechanical strain effect. In Meeting Abstracts (No. 4, pp. 407–407). The Electrochemical. Society (2016)
11. N. Kuwata, N. Iwagami, Y. Matsuda, Y. Tanji, J. Kawamura, Thin film batteries with Li_3PO_4 solid electrolyte fabricated by pulsed laser deposition. ECS Trans. **16**(26), 53–60 (2009)
12. H. Huang, S.C. Yin, T. Kerr, N. Taylor, L.F. Nazar, Nanostructured composites: a high capacity, fast rate $Li_3V_2(PO_4)_3$/carbon cathode for rechargeable lithium batteries. Adv. Mater. **14**(21), 1525–1528 (2002)
13. E. Hosono, T. Kudo, I. Honma, H. Matsuda, H. Zhou, Synthesis of single crystalline spinel $LiMn_2O_4$ nanowires for a lithium ion battery with high power density. Nano Lett. **9**(3), 1045–1051 (2009)
14. B. Kumar, J. Kumar, R. Leese, J.P. Fellner, S.J. Rodrigues, K.M. Abraham, A solid-state, rechargeable, long cycle life lithium–air battery. J. Electrochem. Soc. **157**(1), A50–A54 (2010)
15. N. Ohta, K. Takada, L. Zhang, R. Ma, M. Osada, T. Sasaki, Enhancement of the high-rate capability of solid-state lithium batteries by nanoscale interfacial modification. Adv. Mater. **18**(17), 2226–2229 (2006)
16. C. Guan, W. Zhao, Y. Hu, Q. Ke, X. Li, H. Zhang, J. Wang, High-performance flexible solid-state Ni/Fe battery consisting of metal oxides coated carbon cloth/carbon nanofiber electrodes. Adv. Energy Mater. (2016). doi:10.1002/aenm.201601034
17. G. Tan, F. Wu, C. Zhan, J. Wang, D. Mu, J. Lu, K. Amine, Solid-state li-ion batteries using fast, stable, glassy nanocomposite electrolytes for good safety and long cycle-life. Nano Lett. **16**(3), 1960–1968 (2016)
18. A. Bünting, S. Uhlenbruck, D. Sebold, H.P. Buchkremer, R. Vaßen, Three-dimensional, fibrous lithium iron phosphate structures deposited by magnetron sputtering. ACS Appl. Mater. Interfaces **7**(40), 22594–22600 (2015)
19. N.I. Ayu, E. Kartini, L.D. Prayogi, M. Faisal, Crystal structure analysis of Li_3PO_4 powder prepared by wet chemical reaction and solid-state reaction by using X-ray diffraction (XRD). Ionics **22**(7), 1051–1057 (2016)
20. S.Q. Zhang, S. Xie, C.H. Chen, Fabrication and electrical properties of Li_3PO_4-based composite electrolyte films. Mater. Sci. Eng. **121**(1), 160–165 (2005)
21. L.D. Prayogi, M. Faisal, E. Kartini, W. Honggowiranto, Supardi, *Morphology and conductivity study of solid electrolyte Li_3PO_4, AIP Conference Proceedings Vol. 1710, No. 1*, ed. by A. Purwanto, A. Nur, F. Rahmawati, E. R. Dyartanti, A. Jumari (AIP Publishing, New York, 2016), p. 030047
22. N. Kuwata, N. Iwagami, Y. Tanji, Y. Matsuda, J. Kawamura, Characterization of thin-film lithium batteries with stable thin-film Li_3PO_4 solid electrolytes fabricated by ArF excimer laser deposition. J. Electrochem. Soc. **157**(4), A521–A527 (2010)
23. G. Sun, H. Wang, P. Li, Z. Liu, Z. Jiang, Response characteristics of a potentiometric CO_2 gas sensor based on Li_3PO_4 solid electrolyte using Au film as the electrodes. J. Appl. Phys. **115**(12), 124505 (2014)
24. G. Calcagno, Silicon anodes for all solid state thin film LIBs by ion beam sputtering deposition, Master Thesis, Universitat Stuttgart (2015)
25. G.K. Kiran, T.R. Penki, P.V. Kamath, N. Munichandraiah, Effect of orientation on the reversible discharge capacity of electrodeposited Cu_2O coatings as lithium-ion battery anodes. J. Solid State Electrochem. **20**(2), 555–562 (2016)
26. N. Karaman, M. Aliefendić, S. Pljuco, D. Kozlica, N. Nalić, F. Korać, S. Gutić, Solid state synthesis and characterization of $LiFePO_4$/C as cathode material for Li-ion batteries. Bull. Chem Technol Bosnia Herzegovina, **45**, 19–22 (2015)
27. Y.W. Denis, C. Fietzek, W. Weydanz, K. Donoue, T. Inoue, H. Kurokawa, S. Fujitani, Study of $LiFePO_4$ by cyclic voltammetry. J. Electrochem. Soc. **154**(4), A253–A257 (2007)
28. S. Pat, S. Özen, V. Şenay, Ş. Korkmaz Optical and surface properties of optically transparent Li_3PO_4 solid electrolyte layer for transparent solid batteries. Scanning (2015). doi:10.1002/sca.21272
29. J. Hämäläinen, J. Holopainen, F. Munnik, T. Hatanpää, M. Heikkilä, M. Ritala, M. Leskelä, Lithium phosphate thin films grown by atomic layer deposition. J. Electrochem. Soc. **159**(3), A259–A263 (2012)
30. H.H. Yudar, S. Pat, Ş. Korkmaz, S. Özen, V. Şenay, Zn/ZnSe thin films deposition by RF magnetron sputtering. J. Mater. Sci. **28**(3), 2833–2837 (2017)
31. A. H. Yildirim, Peksoz Characterization of non-vacuum $CuIn_xGa_{1-x}Se_2$ thin films prepared by low-cost sequential electrodeposition technique. Thin Solid Films **631**, 34–40 (2017)